Food Science of Animal Resources

Food Sci. Anim. Resour. 2021 May 41(3):497~508
DOI https://doi.org/10.5851/kosfa.2021.e13

pISSN : 2636-0772 eISSN : 2636-0780
http://www.kosfaj.org

ARTICLE

Therapeutic Effects of *Gleditsia sinensis* Thorn Extract Fermented by *Lactobacillus casei* 3260 in a Type II Collagen-Induced Rheumatoid Arthritis Mouse Model

Ju Young Eor[1,2], Nahyun Park[1], Yoon Ji Son[1,2], and Sae Hun Kim[1,2,*]

[1]College of Life Sciences and Biotechnology, Korea University, Seoul 02841, Korea
[2]Institute of Life Sciences and Natural Resources, Korea University, Seoul 02841, Korea

OPEN ACCESS

Received December 15, 2020
Revised March 5, 2021
Accepted March 21, 2021

***Corresponding author** : Sae Hun Kim
College of Life Sciences and Biotechnology, Korea University, Seoul 02841, Korea
Tel: +82-2-3290-3055
Fax: +82-2-3290-3499
E-mail: saehkim@korea.ac.kr

***ORCID**
Ju Young Eor
https://orcid.org/0000-0002-3764-3339
Nahyun Park
https://orcid.org/0000-0003-4732-8671
Yoon Ji Son
https://orcid.org/0000-0002-5491-2959
Sae Hun Kim
https://orcid.org/0000-0002-0990-2268

Abstract This study aimed to assess the anti-inflammatory effect of *Lactobacillus casei* 3260 (LC) alone and LC-fermented *Gleditsia sinensis* thorn (GST) extract in mouse model of type II collagen induced rheumatoid arthritis (RA). In our previous work, we confirmed the anti-inflammatory effects of LC and GST against LPS-induced inflammation *in vitro*. In this study, LC and GST were fermented and their effects were assessed in an animal model of RA. Both LC and fermented GST (fGST) treatment reduced mice serum nitrite and total cholesterol and triggered myeloperoxidase (MPO) activity. In addition, both LC and fGST reduced inflammation-related serum biomarkers such as tumor necrosis factor-α, interleukin (IL)-6, IL-17, and IL-1β. As per the morphological analysis, both LC and fGST protected hind paw joints against RA, and its related mRNA markers improved. Finally, arthritis scores were measured as an indicator of RA of the whole experimental period; the scores suggested that both LC and fGST protect against collagen-induced RA-related inflammation in a mouse model.

Keywords *Lactobacillus*, *Gleditsia sinensis*, fermentation, rheumatoid arthritis, tacrolimus

Introduction

Rheumatoid arthritis (RA) is a chronic systemic autoimmune disease that occurs more frequently in females than in males, being predominantly observed in the elderly (Guo et al., 2018). RA has various symptoms such as articular pain, cartilage degradation, bone destruction, and functional disability (Rudbane et al., 2018). In particular, RA treatment includes the use of both conventional and biological therapeutics such as tumor necrosis factor (TNF) inhibitors (certolizumab, golimumab, adalimumab, and infliximab) and biosimilars and small oral molecules (tofacitinib, upadacitinib, and baricitinib). However, anti-TNF-α treatment is discontinued in approximately 30%–40% of patients owing to primary failure problem, secondary loss of response, or intolerance (Rubbert-Roth et al., 2019). Meanwhile, there is a growing awareness that the gut microbiome (GM) plays an essential role in the RA improvement and advancement. The gut-associated lymphoid tissue (GALT) works with the GM on maintaining immune system homeostasis and perform as a marker of the health condition of host (Achi et al., 2019).

Probiotics are living microorganisms, which upon consumption in adequate amounts can improve the health of an individual. Metabolites as vitamins and short chain fatty acids can be produced by probiotic strains and are energy sources for the intestinal cells. In addition, these may improve the GM and intestinal immune system to maintain gut health. Recently, probiotics such as *Lactobacillus rhamnosus*, *L. casei*, *L. reuteri*, *L. acidophilus*, *Bacillus coagulans*, and *Bifidobacterium bifidum* have been studied for their potential to treat RA in randomized controlled trials. These probiotics have been shown to be safe and effective in patients with RA (Bodkhe et al., 2019). In these reasons, we used *L. casei* 3260 as probiotic strain which has been previously reported to have anti-inflammatory effect by inhibiting both cyclooxygenase-2, and nuclear factor-kappaB (NF-κB) in other institute (Lee et al., 2008).

Gleditsia sinensis Lam. thorn (GST) has long been used in traditional medicine for the treatment in early stage of carbuncle, unbroken ulceration, swelling, and skin diseases (Wang et al., 2018). The chemical compounds of GST possess a wide spectrum of therapeutic activities such as anti-inflammatory, anti-oxidant, anti-microbial, and anti-tumor effects (Kim et al., 2015).

The aim of this study was to assess the therapeutic effects of *Lactobacillus casei* 3260 (LC), as a probiotic, and those of herbal chemical compounds from LC-fermented GST (fGST) by measuring NO and TNF-α expression levels in LPS-stimulated murine macrophage RAW 264.7 cells. In addition, we evaluated the therapeutic effects of LC and fGST by analyzing the bone metabolism- and pro-inflammatory cytokine-related mRNA expression in a mouse model of RA induced by injecting bovine type II collagen in DBA/1 mice.

Materials and Methods

Preparation of GST methanol extract

The GST was purchased from Kyung-dong market (Seoul, Korea); it was extracted using methanol as the medium. The protocol of extraction was obtained from the Natural Product and Metabolomics Lab (Seoul, Korea University). The extracted sample was then directly used for the experiments.

Preparation of the probiotic strain

L. casei 3260 was obtained from Korean Collection for Type Culture (KCTC, Jeongeup, Korea). The strain was delivered in frozen state; therefore, the samples were activated by inoculating 1% (v/v) strain thrice in De Man Rogosa Sharpe (MRS) medium (Difco, Detroit, MI, USA) at 37°C for 24 h prior to initiating each cell and animal studies.

Preparation of fGST extract

L. casei 3260 and GST were used to prepare fGST. *L. casei* 3260 was inoculated in 1% (v/v) GST extract, and the samples were then incubated at 37°C for 18 h. After fermentation, fGST was centrifuged to obtain a supernatant. The supernatant was then freeze-dried, powdered, and stored at –80°C for future use.

Animals

The Korea University Institutional Animal Care & Use Committee, Korea (KUIACUC-2017-39) approved this experiment. Six-week-old normal male DBA/1 mice (n=70) were provided by Orient Bio (Seongnam, Korea). The mice were then caged in a cage for 1 week. Standard diet, controlled environmental background, and water *ad libitum* (24±0.5°C, 50%–60% relative humidity, 12-h light/dark cycle) were provided.

Preparation of chemical reagents and assessment of RA

Following protocol from Bendele (2001) and Stasiuk et al. (1996), the RA was induced by injecting bovine type II collagen (CII) to mice, CII was dissolved in 0.1 M acetic acid at 2 mg/mL overnight at 4°C, after which the solution was emulsified in an equal volume of complete Freund's adjuvant (CFA) (Chondrex, Washington, DC, USA) containing 2 mg/mL of freeze-dried powder form of *Mycobacterium tuberculosis*. This emulsion containing 100 mg of CII was injected into the base of the tail (day 7), and mice were boosted using the same schedule 14 days later (day 21). To assess the severity of arthritis in mice, all paws were scored from 0 to 4 (0, normal; 1, mild swelling confined to the tarsals; 2, swelling of two or more toes or joints, or increased swelling; 3, moderate swelling extending from the ankle to the metatarsal joints; and 4, severe swelling encompassing the ankle, foot, and digits). The data were then represented by the sum of the scores of all four paws (Jung et al., 2017).

Treatment protocol

DBA/1 mice were allocated into six groups (n=10): G1=Normal control (Con); G2=RAs; G3=RA mice treated with FK 506 (5 mg/kg) (FK506); G4=RA mice treated with *L. casei* 3260 (1×10^8 CFU/g/day) (LC); G5=RA mice treated with GST (20 mg/kg) (GST); and G6=RA mice treated with fGST (20 mg/kg) (fGST). Each treatment was orally gavaged once daily for 2 weeks. Meanwhile, CII treatment was initiated with intraperitoneal (i.p.) injection after the adjustment period. Weight of all mice was measured twice a week. Each mice were then sacrificed by cervical sprain after placing them into a CO_2 chamber for 2 min at the end of experiment (Fig. 1).

Quantitative reverse transcription (qRT)-PCR analysis

The expression of the mRNA in the serum and samples of femur were analyzed using qRT-PCR. Shortly, using TRIzol reagent (Invitrogen, Carlsbad, CA, USA) with following the protocol, the RNA was extracted. Using a NanoDrop spectrophotometer (Thermo Fisher Scientific, Wilmington, MA, USA), the concentration of RNA was then evaluated. And using a high-capacity cDNA reverse transcription kit (Applied Biosystems, Foster City, CA, USA), the 20 μL of reverse transcription was reacted with the mixture. The PCR mixtures were then mixed with MG 2X qPCR MasterMix (SYBR green)

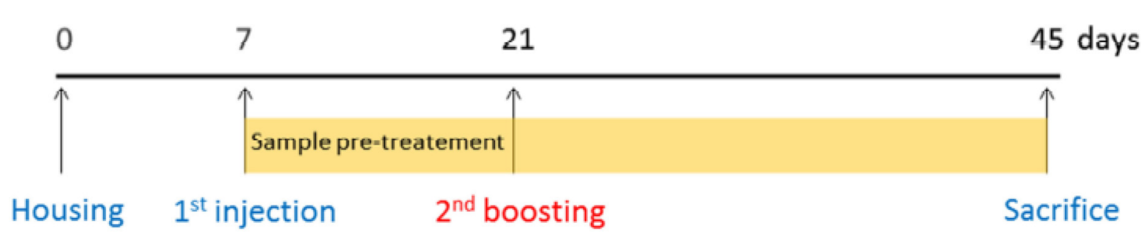

Fig. 1. Graphical abstract of the experiment.

(MGmed, Seoul, Korea) following manufacturer's protocol. After gene amplifying, the samples were analyzed with CFX96™ RT PCR machine (Bio-Rad, Hercules, CA, USA). The β-actin as the housekeeping gene. The expression of mRNA levels each genes of analyzed samples were analyzed with calculation using Bio-Rad CFX manager software (Bio-Rad) (Eor et al., 2020).

Serum biochemical analysis

Mice blood samples syringed in BD Vacutainer^{TM} SST tube (BD, Franklin Lakes, NJ, USA) through cardiac puncture after CO_2 inhalation. Following the collection, the samples were incubated at 25°C for 25 min and centrifuged at 12,000×g for 15 min at 25°C. The supernatant of the samples were collected and indicated as the serum sample. All serum samples were stored at –80°C before using for biochemical analysis. Serum NO was measured using the nitrate/nitrite colorimetric assay kit (Cayman Chemical, Ann Arbor, MI, USA). Assays were performed as per the manufacturers' protocols. Serum TNF-α was measured using the mice TNF-α ELISA kit (Koma Biotech, Seoul, Korea) referring the added protocol. The levels of total triglyceride (TG) and total cholesterol (TC) in serum samples were analyzed with colorimetric enzymatic kits (Embiel, Gunpo, Korea) following manufacturer's procedure. Absorbance of samples in each analysis was then measured using VersaMax^{TM} microplate spectrophotometer (Molecular Device, San Jose, CA, USA).

Clinical scoring analysis

The evaluation of RA progression and severity was analyzed twice a week. The each group of mouse paw was observed by more than three researchers and scored in some criteria from 0 to 4 with graded scale following method from previous research (Baharav et al., 2004). Each paw phenotypic changes were assessed. The result from one mice may be maximum score of 16. Clinical severity score was also assessed in a same way in the ankle thickness with calipers of each paw. Total clinical assessments were evaluated in a blinded manner.

Histological analysis

All hind paw samples were disected after sacrifice. The samples were then fixed with formalin 10% (v/v) after put into embedding cassettes (Simport Scientific, Québec, QU, Canada) for 24 h at 25°C. The synovium analysis with immunohistochemical staining was performed. The 5-μm thickness samples embedded with paraffin blocks was put in formalin. The sections were mounted in glass slides. The samples were then de-paraffinized in xylene. In the next step, the samples were re-hydrated in a series of ethanol. And the samples took microwave antigen (Ag) retrieval. The activity of endogenous peroxidase was inhibited with 3% hydrogen peroxide. After inhibition of the binding with putting the samples with 10% goat serum at 37°C for 60 min, the samples were then stored at 4°C with a 10^{-2} dilution of mouse anti-human calcineurin antibody (Ab) (Sigma-Aldrich, St. Louis, MO, USA). The slides were diluted and stored with secondary Ab known as biotinylated goat anti-mouse IgG (Agilent, Santa Clara, CA, USA). After all steps, the samples were put with peroxidase-conjugated streptavidin at 25°C for 30 min. To reveal Ag, 3,3-diaminobenzidine was added. The samples were counter-stained with Mayer hematoxylin. After that, cleaned, dehydrated, and mounted. In the same manner as described above, the negative control was also prepared without primary Ab was eliminated or changed with isotype control Ab (IgG1; R&D Systems, Minneapolis, MN, USA). All dyed and captured sections were then assessed using scoring method following grades as 0: no abnormality, 1: minimum (<1%), 2: medium (1%–25%), 3: moderate (26%–50%), 4: marked (51%–75%), and 5: severe (76%–

100%) detection following method from Balkrishna et al. (2019) and cartilage score from Mauri et al. (2000).

Statistical analysis

Data were analyzed statistically using IBM SPSS Statistics software version 24.0 (IBM, New York, NY, USA). One-way analysis of variance was used to analyze the statistical difference between sample means. The statistical significance level was defined as α=0.05. The multiple comparisons of means were assessed by Tukey's tests.

Results and Discussion

Biochemical analysis in serum

The mouse serum was analyzed as demonstrated in Fig. 2. The results indicate the effect of each treatment toward four serum profiles, which act as downstream response of RA. TG levels were constant after RA induction compared to those in the control group (Fig. 2A). Although TC levels were not significantly different after RA induction compared to those in the control group, three different treatments including either probiotics or GST, especially in fGST group, significantly reduced TC levels (Fig. 2B). In humans, TC levels increase in RA; therefore, RA can be predicted before the critical symptoms are initiated (Turesson et al., 2015). The serum NO level is a biomarker of rheumatoid NO and increase in inflammatory

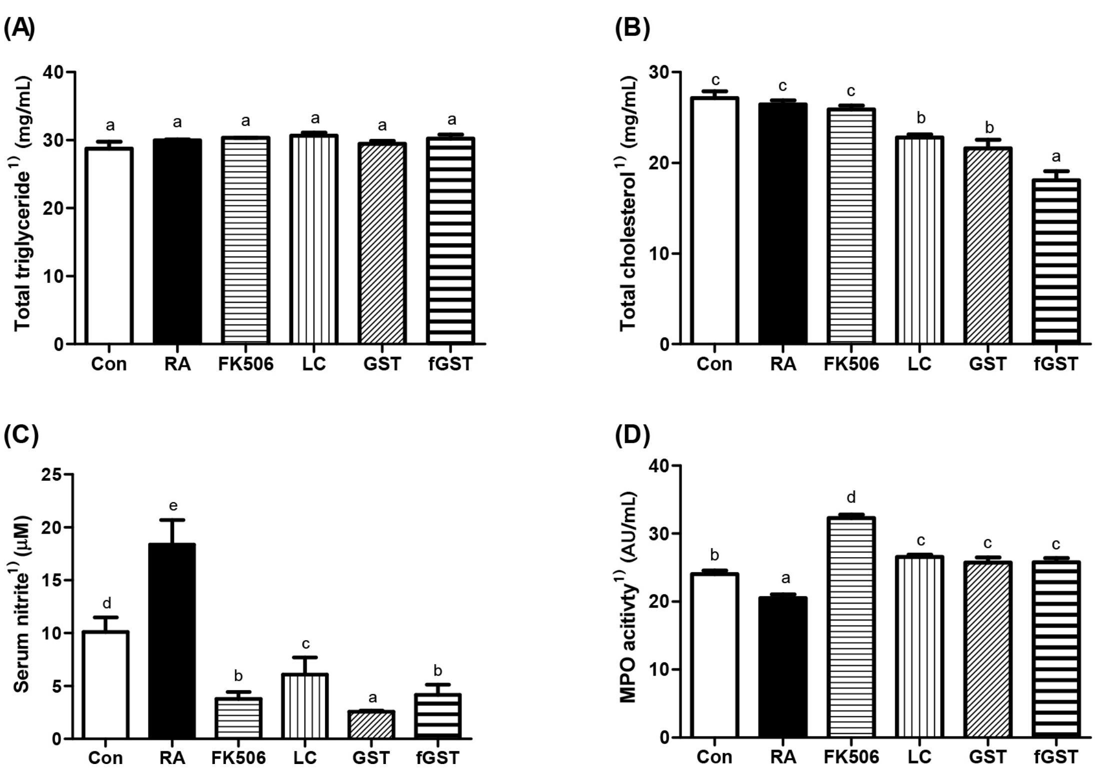

Fig. 2. Effect of each treatment on serum (A) total triglyceride (TG), (B) total cholesterol (TC), (C) nitrite levels, and (D) Myeloperoxidase (MPO) activity in rheumatoid arthritis (RA)-induced mice. [1)] Results were expressed as mean±SEM (n=5). [a–e] Means with different lowercase superscript letters are significantly different (p<0.05). Con, normal control group; RA, rheumatoid arthritis induced group; FK506, rheumatoid arthritis induced mice treated with FK 506 group; LC, rheumatoid arthritis induced mice treated with *L. casei* 3260 group; GST, rheumatoid arthritis induced mice treated with *Gleditsia sinensis* thorn group; Rheumatoid arthritis induced mice treated with fermented *Gleditsia sinensis* thorn group; fGST, fermented GST.

conditions (Garg et al., 2017). All treatments severely elevated serum NO levels in RA-induced mice; the levels were most dramatically declined in the GST group among the four different treatments (Fig. 2C). Moreover, myeloperoxidase (MPO) levels were significantly low after RA induction, but each treatment restored MPO activity against RA induction (Fig. 2D); restoration of MPO activity was previously indicated as the anti-oxidative and anti-inflammatory activity (Eor et al., 2020).

Inflammatory cytokine measurement in serum

Effect of treatments on serum inflammatory cytokines level are shown in Fig. 3. TNF-α is an inflammatory cytokine in the serum and may also be the indicator of severity of inflammation (Bautista-Herrera et al., 2018). In our experiments, TNF-α level was dramatically increased by RA induction, and these elevations were recovered by either FK506 medication or each treatment (Fig. 3A). Previous reports suggest that interleukin (IL)-6 blockade may be the clinical target of patients with RA (Narazaki et al., 2017). IL-17 is also closely related to RA as it mediates mitochondrial functions (Kim et al., 2017). Therefore, we measured IL-6, IL-17, and IL-1β levels in the serum. Similar to the increase in TNF-α concentration levels, the levels of IL-6, IL-17, and IL-1β rapidly increased in the RA group, and then were attenuated by the four different treatments (Fig. 3B, 3C, and 3D). Interestingly, fGST group showed significant improvement in both IL-6 and IL-1β. This amelioration can be compared to sole treatment of GST by mitigating concentrations comparable to control group, respectively.

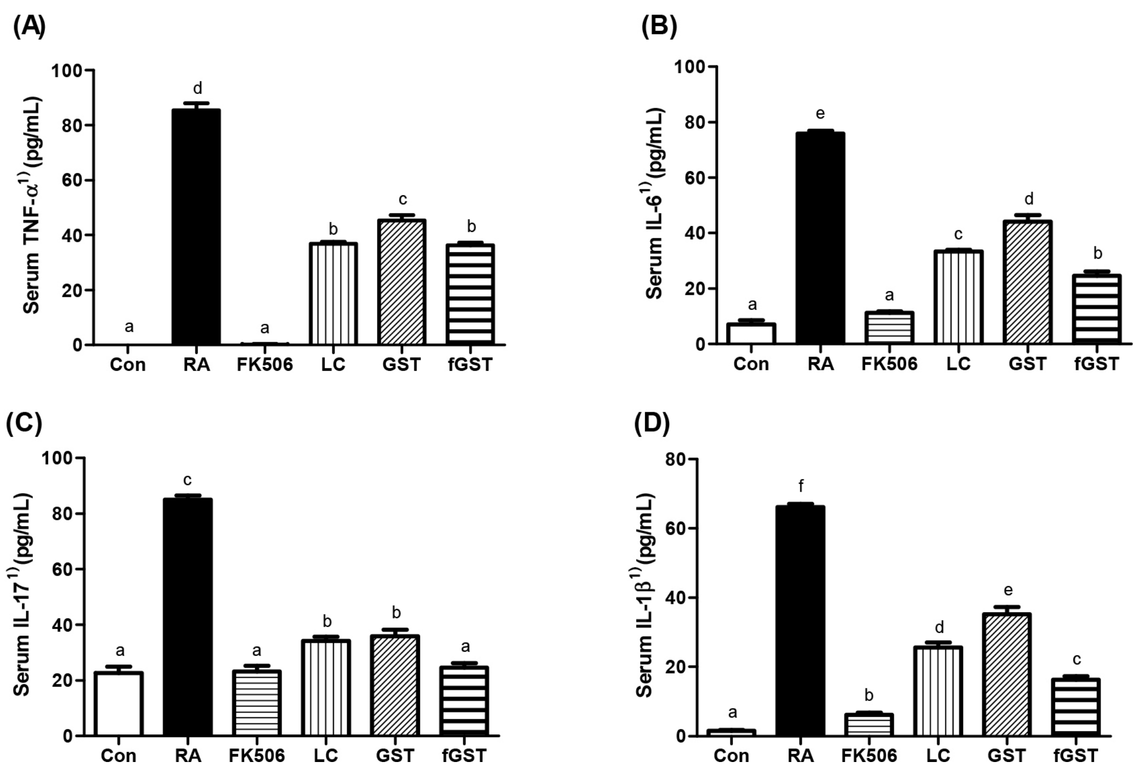

Fig. 3. Effect of each treatment on serum levels of (A) tumor necrosis factor (TNF)-α, (B) interleukin (IL)-6, (C) IL-17, and (D) IL-1β in rheumatoid arthritis (RA)-induced mice. [1)] Results were expressed as mean±SEM (n=5). [a–f] Means with different lowercase superscript letters are significantly different (p<0.05). Con, normal control group; RA, rheumatoid arthritis induced group; FK506, rheumatoid arthritis induced mice treated with FK 506 group; LC, rheumatoid arthritis induced mice treated with *L. casei* 3260 group; GST, rheumatoid arthritis induced mice treated with *Gleditsia sinensis* thorn group; Rheumatoid arthritis induced mice treated with fermented *Gleditsia sinensis* thorn group; fGST, fermented GST.

Morphologic analysis of hind paw joints in mice

To analyze the protective effect of each treatments, three different kinds of staining were performed on the hind paw joints in mice (Fig. 4). First, H&E staining was performed to assess whether each treatment showed joint morphological differences. Severe disruption of cartilage in was observed in the RA group compared to that in the control group, and the disruption was recovered in FK506, LC, GST, and fGST groups. The fGST group showed a similar state as the FK506 group (Fig. 4A). A

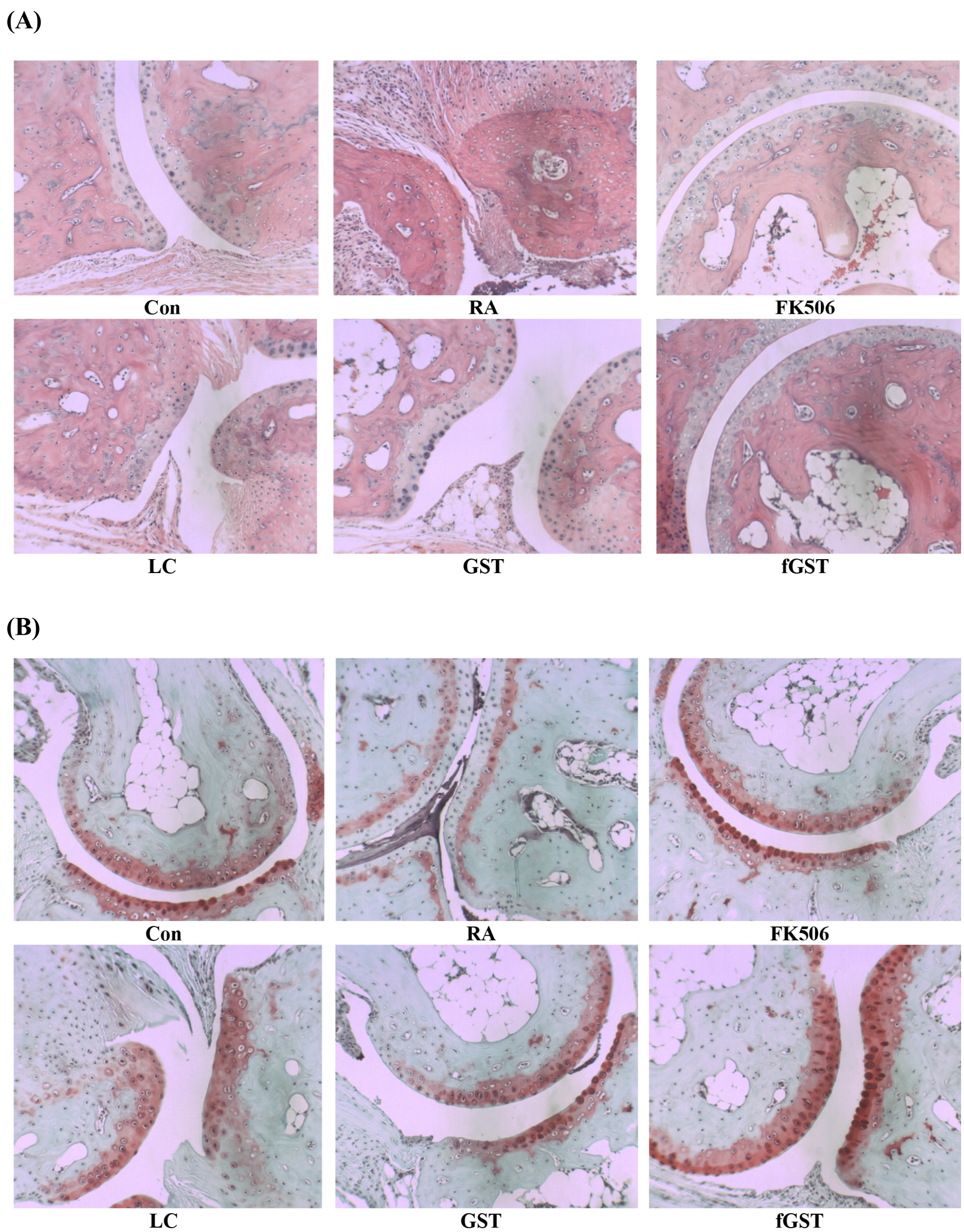

Fig. 4. Histological analysis of the hind-paw joints of rheumatoid arthritis (RA)-induced mice at day 45. (A) Hematoxylin and eosin (H&E)-, (B) safranin-O-, (C) calcineurin-stained sections (100×, respectively), and (D) section lesion score and cartilage damage of total staining. [1)] Results were expressed as mean±SEM (n=5). [a–e] Means with different lowercase superscript letters are significantly different ($p<0.05$). Con, normal control group; RA, rheumatoid arthritis induced group; FK506, rheumatoid arthritis induced mice treated with FK 506 group; LC, rheumatoid arthritis induced mice treated with *L. casei* 3260 group; GST, rheumatoid arthritis induced mice treated with *Gleditsia sinensis* thorn group; Rheumatoid arthritis induced mice treated with fermented *Gleditsia sinensis* thorn group; fGST, fermented GST.

(C)

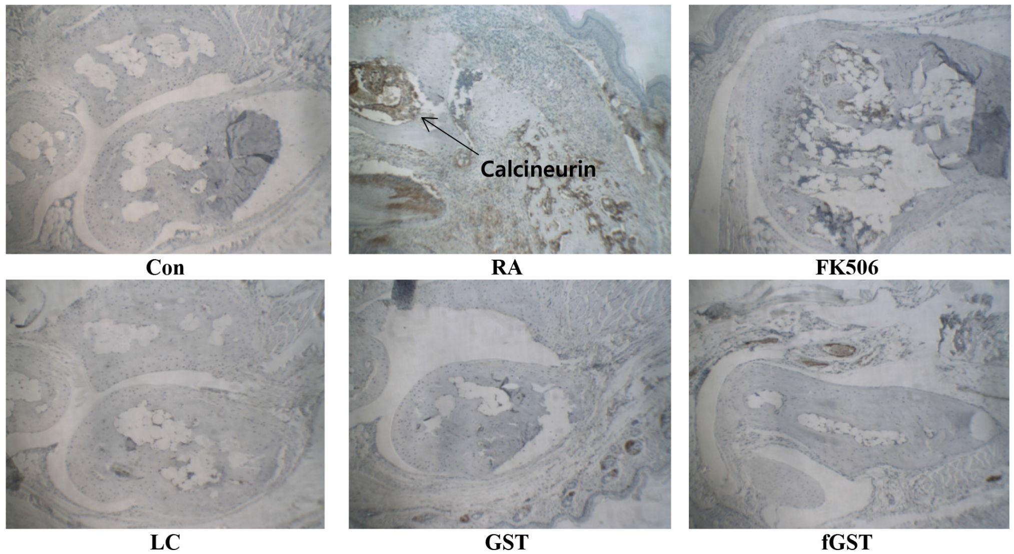

(D)

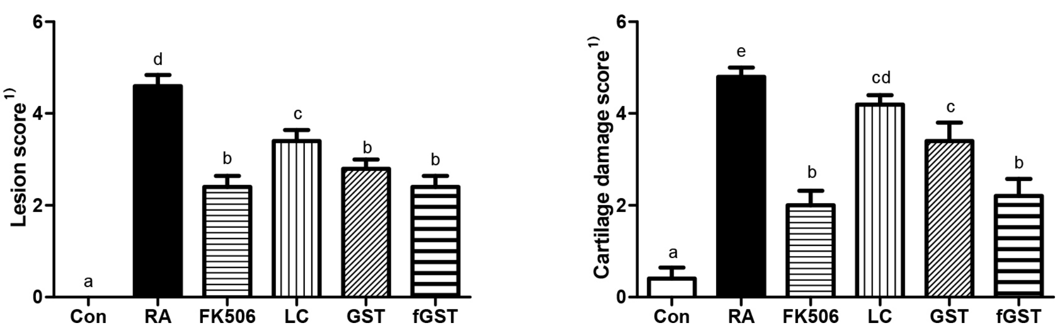

Fig. 4. Histological analysis of the hind-paw joints of rheumatoid arthritis (RA)-induced mice at day 45 (continued). (A) Hematoxylin and eosin (H&E)-, (B) safranin-O-, (C) calcineurin-stained sections (100×, respectively), and (D) section lesion score and cartilage damage of total staining. [1)] Results were expressed as mean±SEM (n=5). [a–e] Means with different lowercase superscript letters are significantly different (p<0.05). Con, normal control group; RA, rheumatoid arthritis induced group; FK506, rheumatoid arthritis induced mice treated with FK 506 group; LC, rheumatoid arthritis induced mice treated with *L. casei* 3260 group; GST, rheumatoid arthritis induced mice treated with *Gleditsia sinensis* thorn group; Rheumatoid arthritis induced mice treated with fermented *Gleditsia sinensis* thorn group; fGST, fermented GST.

previous study reported that a neutrophil extracellular trap may enhance the cartilage component in an RA model, and thus, the cartilage was analyzed using safranin-O staining (Carmona-Rivera, 2020). Similarly, we used safranin-O staining to further investigate whether each treatment had any effects on cartilage integrity. The results indicated that cartilage integrity was weakened in the RA group, represented by the diminished red area compared to that in the control group (Fig. 4B). However, this disorganization was reversed after the four different treatments which restored the red areas in the cartilage (Fig. 4B). Calcineurin is increased in the patient joints with RA with inflammation (Yoo et al., 2006). Therefore, calcineurin staining was performed in the joints of the mice. The RA group showed the highest expression of calcineurin after the stained samples were incubated with calcineurin antibodies, whereas the elevated level of calcineurin was reduced by FK506 medication, and especially attenuated by LC, GST, and fGST (Fig. 4D). From the histologic scoring analysis, both lesion score and cartilage damge were restored after both GST and fGST group compared to RA group (Mauri et al., 2000).

qPCR analysis of hind paw joint in mice

Osteoporosis and RA are related to the OPG and RANKL balance, which is responsible for bone formation and absorption through OPG/RANKL/NF-κB signaling pathways (Zhao et al., 2021). Fig. 5 shows the effect of each treatment on mRNA expression in hind paw joint of RA-induced mice. mRNA expression of OPG was increased in the RA group, and the treatments failed to mitigate the increase. RANKL expression also worsened in the RA group. Unlike the expression of OPG, all treatments diminished the mRNA expression of RANKL compared to that in the RA group without treatment. Similar to the serum level of inflammatory cytokines, the mRNA expression of IL-6 was elevated by RA induction. This is the parallel to the study by Pandolfi et al. (2020). The increase was attenuated by each treatment; it was especially declined in the fGST group. The mRNA expression of IL-8 and IL-17 showed a tendency similar to that of IL-6, which was increased by RA induction and most significantly attenuated in the fGST group (Lin et al., 2019).

Arthritis score analysis

The arthritis score after each treatment is shown on Fig. 6. While the control group showed constant zero score of arthritis, RA induction initiated the symptoms at day 22 and they increased constantly. Although every treatment showed initiation at day 22 and continually increasing clinical score, each elevation of severity was hindered compared to RA group. Interestingly, the clinical score declined at day 41 of fGST treatment, whereas other treatments demonstrated gradually increasing severity.

Conclusion

This study was designed to assess the protective effect of either *Lactobacillus* strain or fGST in a mouse model of RA. Serum biochemical profiles and anti-inflammatory cytokine levels were improved by administrating each treatment ($p<0.05$). Moreover, three different morphological analyses of hind paw joints of mice suggested that each treatment may have joint-

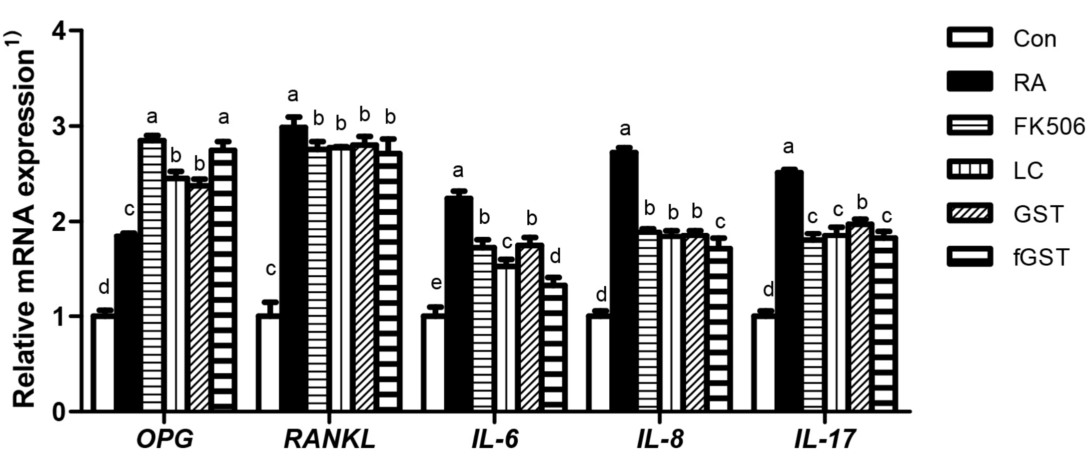

Fig. 5. Effect of each treatment on the mRNA expression levels of targeted genes in the hind-paw joints of rheumatoid arthritis (RA)-induced mice at day 45. [1)] Results were normalized to the control group, and expressed as mean±SEM (n=5). [a–d] Means with different lowercase superscript letters are significantly different ($p<0.05$). Con, normal control group; RA, rheumatoid arthritis induced group; FK506, rheumatoid arthritis induced mice treated with FK 506 group; LC, rheumatoid arthritis induced mice treated with *L. casei* 3260 group; GST, rheumatoid arthritis induced mice treated with *Gleditsia sinensis* thorn group; Rheumatoid arthritis induced mice treated with fermented *Gleditsia sinensis* thorn group; fGST, fermented GST.

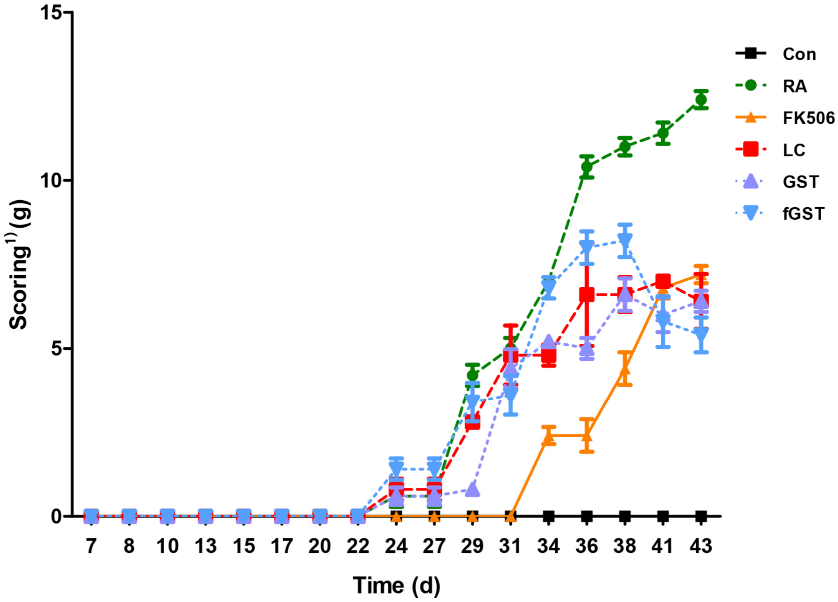

Fig. 6. Arthritis scores in rheumatoid arthritis (RA)-induced mice administered *Gleditsia sinensis* Lam. thorn (GST) extract, probiotic bacteria, or fermentation. 1) Beginning 14 days before secondary immunization, mice received each treatment with one of four therapies: FK506 (5 mg/kg) (FK506), *L. casei* 3260 (1×10^8 CFU/g/day) (LC), GST (20 mg/kg) (GST), and fermented GST (20 mg/kg) (fGST). Each treatment was orally gavaged once daily for 2 weeks. Con, normal control group; RA, rheumatoid arthritis induced group; FK506, rheumatoid arthritis induced mice treated with FK 506 group; LC, rheumatoid arthritis induced mice treated with *L. casei* 3260 group; GST, rheumatoid arthritis induced mice treated with *Gleditsia sinensis* thorn group; Rheumatoid arthritis induced mice treated with fermented *Gleditsia sinensis* thorn group; fGST, fermented GST.

protective effect by lowering cartilage damage against RA induction. In parallel to morphologic analysis, qPCR results also showed the protective effect of the three treatments by normalizing OPG and RANKL balance and alleviating IL-6, IL-7, and IL-8 levels ($p<0.05$). Finally, the daily arthritis scoring further confirmed the protective effect of the treatments against RA ($p<0.05$), and this may be related to the alleviation of serum IL-6 and IL-17 (Haleagrahara et al., 2017). According to all implications and suggestions from the results, the administration of *L. casei* 3260, GST, and fGST may have the therapeutic potential to cure RA.

Conflicts of Interest

The authors declare no potential conflicts of interest.

Acknowledgements

This work was supported by a grant from the Institute of Life Science and Natural Resources, Korea University.

Author Contributions

Conceptualization: Park N. Data curation: Eor JY, Park N. Formal analysis: Eor JY, Park N. Methodology: Park N. Software: Park N. Validation: Eor JY. Investigation: Eor JY. Writing - original draft: Eor JY. Writing - review & editing: Eor N, Park N, Son YJ, Kim SH.

Ethics Approval

The experiment was approved by the Korea University Institutional Animal Care & Use Committee, Korea (KUIACUC-2017-39).

References

Achi SC, Talahalli RR, Halami PM. 2019. Prophylactic effects of probiotic *Bifidobacterium* spp. in the resolution of inflammation in arthritic rats. Appl Microbiol Biotechnol 103:6287-6296.

Baharav E, Mor F, Halpern M, Weinberger A. 2004. *Lactobacillus* GG bacteria ameliorate arthritis in Lewis Rats. J Nutr 134:1964-1969.

Balkrishna A, Sakat SS, Joshi K, Paudel S, Joshi D, Joshi K, Ranjan R, Gupta A, Bhattacharya K, Varshney A. 2019. Anti-inflammatory and anti-arthritic efficacies of an Indian traditional herbo-mineral medicine "Divya Amvatari Ras" in collagen antibody-induced arthritis (CAIA) mouse model through modulation of IL-6/IL-1*β*/TNF-*α*/nf*κ*b signaling. Front Pharmacol 10:659.

Bautista-Herrera LA, De la Cruz-Mosso U, Morales-Zambrano R, Villanueva-Quintero GD, Hernández-Bello J, Ramírez-Dueñas MG, Martínez-López E, Brennan-Bourdon LM, Baños-Hernández CJ, Muñoz-Valle JF. 2018. Expression of MIF and TNFA in psoriatic arthritis: Relationship with Th1/Th2/Th17 cytokine profiles and clinical variables. Clin Exp Med 18:229-235.

Bendele AM. 2001. Animal models of rheumatoid arthritis. J Musculoskelet Neuronal Interact 1:377-385.

Bodkhe R, Balakrishnan B, Taneja V. 2019. The role of microbiome in rheumatoid arthritis treatment. Ther Adv Musculoskelet Dis 11:1759720X19844632.

Carmona-Rivera C, Carlucci PM, Goel RR, James E, Brooks SR, Rims C, Hoffmann V, Fox DA, Buckner JH, Kaplan MJ. 2020. Neutrophil extracellular traps mediate articular cartilage damage and enhance cartilage component immunogenicity in rheumatoid arthritis. JCI Insight 5:e139388.

Eor JY, Tan PL, Son YJ, Lee CS, Kim SH. 2020. Milk products fermented by *Lactobacillus* strains modulate the gut-bone axis in an ovariectomised murine model. Int J Dairy Technol 73:743-756.

Garg N, Syngle A, Krishan P. 2017. Nitric oxide: Link between inflammation and endothelial dysfunction in rheumatoid arthritis. Int J Angiol 26:165-169.

Guo Q, Wang Y, Xu D, Nossent J, Pavlos NJ, Xu J. 2018. Rheumatoid arthritis: Pathological mechanisms and modern pharmacologic therapies. Bone Res 6:1-14.

Haleagrahara N, Miranda-Hernandez S, Alim MA, Hayes L, Bird G, Ketheesan N. 2017. Therapeutic effect of quercetin in collagen-induced arthritis. Biomed Pharmacother 90:38-46.

Jung H, Jung SM, Rim YA, Park N, Nam Y, Lee J, Park SH, Ju JH. 2017. Arthritic role of *Porphyromonas gingivalis* in collagen-induced arthritis mice. PLOS ONE 12:e0188698.

Kim EK, Kwon JE, Lee SY, Lee EJ, Kim DS, Moon SJ, Lee J, Kwok SK, Park SH, Cho ML. 2017. IL-17-mediated mitochondrial dysfunction impairs apoptosis in rheumatoid arthritis synovial fibroblasts through activation of autophagy. Cell Death Dis 8:e2565.

Kim Y, Koh JH, Ahn YJ, Oh S, Kim SH. 2015. The synergic anti-inflammatory impact of *Gleditsia sinensis* Lam. and *Lactobacillus brevis* KY21 on intestinal epithelial cells in a DSS-induced colitis model. Korean J Food Sci Anim Resour

35:604-610.

Lee JM, Hwang KT, Jun WJ, Park CS, Lee MY. 2008. Antiinflammatory effect of lactic acid bacteria: Inhibition of cyclooxygenase-2 by suppressing nuclear factor-*κB* in Raw264.7 macrophage cells. J Microbiol Biotechnol 18:1683-1688.

Lin J, He Y, Wang B, Xun Z, Chen S, Zeng Z, Ou Q. 2019. Blocking of YY1 reduce neutrophil infiltration by inhibiting IL-8 production via the PI3K-Akt-mTOR signaling pathway in rheumatoid arthritis. Clin Exp Immunol 195:226-236.

Mauri C, Mars LT, Londei M. 2000. Therapeutic activity of agonistic monoclonal antibodies against CD40 in a chronic autoimmune inflammatory process. Nat Med 6:673-679.

Narazaki M, Tanaka T, Kishimoto T. 2017. The role and therapeutic targeting of IL-6 in rheumatoid arthritis. Expert Rev Clin Immunol 13:535-551.

Pandolfi F, Franza L, Carusi V, Altamura S, Andriollo G, Nucera E. 2020. Interleukin-6 in rheumatoid arthritis. Int J Mol Sci 21:5238.

Rubbert-Roth A, Szabó MZ, Kedves M, Nagy G, Atzeni F, Sarzi-Puttini P. 2019. Failure of anti-TNF treatment in patients with rheumatoid arthritis: The pros and cons of the early use of alternative biological agents. Autoimmun Rev 18:102398.

Rudbane SMA, Rahmdel S, Abdollahzadeh SM, Zare M, Bazrafshan A, Mazloomi SM. 2018. The efficacy of probiotic supplementation in rheumatoid arthritis: A meta-analysis of randomized, controlled trials. Inflammopharmacology 26:67-76.

Stasiuk LM, Abehsira-Amar O, Fournier C. 1996. Collagen-induced arthritis in DBA/1 mice: Cytokine gene activation following immunization with type II collagen. Cell Immunol 173:269-275.

Turesson C, Bergström U, Pikwer M, Nilsson JA, Jacobsson LTH. 2015. High serum cholesterol predicts rheumatoid arthritis in women, but not in men: A prospective study. Arthritis Res Ther 17:284.

Wang L, Hui Y, Jiang K, Yin G, Wang J, Yan Y, Wang Y, Li J, Wang P, Bi K, Wang T. 2018. Potential of near infrared spectroscopy and pattern recognition for rapid discrimination and quantification of *Gleditsia sinensis* thorn powder with adulterants. J Pharm Biomed Anal 160:64-72.

Yoo SA, Park BH, Park GS, Koh HS, Lee MS, Ryu SH, Miyazawa K, Park SH, Cho CS, Kim WU. 2006. Calcineurin is expressed and plays a critical role in inflammatory arthritis. J Immunol 177:2681-2690.

Zhao X, Jiang S, Dong Q, Dang J, Liu Z, Han H, Tao Y, Yue H. 2021. Anti-rheumatoid arthritis effects of iridoid glucosides from *Lamiophlomis rotata* (Benth.) kudo on adjuvant-induced arthritis in rats by OPG/RANKL/NF-κB signaling pathways. J Ethnopharmacol 266:113402.